May 1987 LRP 318/87

TIME-RESOLVED LINEWIDTH AND LINESHAPE MEASUREMENTS OF A PULSED OPTICALLY PUMPED FAR INFRARED D_2O LASER

R. Behn, M.A. Dupertuis, Peter A. Krug, I. Kjelberg
S.A. Salito, M.R. Siegrist

TIME-RESOLVED LINEWIDTH AND LINESHAPE MEASUREMENTS OF A PULSED OPTICALLY PUMPED FAR INFRARED D_2O LASER

R. Behn, M.A. Dupertuis*, Peter A. Krug**, I. Kjelberg***

S.A. Salito, M.R. Siegrist

Centre de Recherches en Physique des Plasmas
Association Euratom - Confédération Suisse
Ecole Polytechnique Fédérale de Lausanne
21, Av. des Bains, CH-1007 Lausanne, Switzerland

Present addresses :

* Research Institute for Theoretical Physics
University of Helsinki, Siltavuorenpenger 20C
SF-00170 Helsinki 17, Finland

** School of Physics, University of Sydney
N.S.W. 2006, Australia

***Norwegian Defence Research Establishment
Division for Electronics, P.O. Box 25
N-2007 Kjeller, Norway

Abstract

The spectral composition of the emission of an optically pumped D_2O FIR laser around the 385μm line has been measured as a function of time during the 1μs pulse duration.

For this purpose a multichannel heterodyne receiver comprising a Schottky barrier diode has been used providing a spectral resolution of 80MHz.

A spectral shift of the laser emission during the pulse has been observed, which is caused by the AC Stark effect, but also other mechanisms seem to play an important role. The emission spectra have been studied as a function of instantaneous pump power and time for different D_2O pressures. Since the D_2O laser contains no frequency selective elements multi-mode emission and mode competition effects lead to a complex behaviour.

Nevertheless an attempt is made to explain the observations on the basis of a theoretical model.

1. INTRODUCTION

In many applications of pulsed optically pumped far infrared (FIR) lasers, spectral purity and stability of the emission frequency are very important. In the case of plasma diagnostics [1, 2] this is essential because the spectral shape of the laser radiation collected after its interaction with the plasma is analysed to obtain information on the plasma parameters and thus should not be influenced by any other effects. However, especially in off-resonantly pumped FIR lasers there are several mechanisms which can lead to chirping or to a time variation of the width of the emission profile. The peaks of the gain profile vary in frequency due to the pump and far infrared laser induced AC Stark effect and also due to saturation mechanisms [3]. If single mode emission is not imposed by external means, mode competition effects also profoundly alter the gain profile.

We report time- and frequency-resolved measurements of the output of an optically pumped D_2O laser at 385μm, using a heterodyne receiver with spectral resolution of 80MHz and a time resolution of 30ns. The experiment was performed using a laser and detection system which were designed for an ion temperature measurement on a tokamak plasma by Thomson scattering, and as such were not optimized for the time- and frequency-resolved measurements reported here. In particular, the 80MHz spectral resolution was insufficient to resolve individual resonator modes. On the other hand the wide total bandwidth of the detection system of about 1 GHz allowed us to observe the whole spectral region around 780GHz within which laser emission can be expected. Since the laser was optimised for long pulse operation

(~1μs) the time resolution mentioned was adequate to follow the temporal evolution during the pulse. We report a wealth of interesting effects, not all of which have so far been explained.

2. THEORETICALLY PREDICTED EFFECTS

The D_2O emission line at 385μm, pumped with the 9R(22) line (9.26μm) of a CO_2 laser, is a well known and extensively studied transition [1, 3, 4, 5]. Unless the CO_2 laser is continuously tunable, which is not the case in this experiment, the CO_2 laser frequency is offset from the line center of the D_2O absorbing transition by about 320MHz. Hence pumping takes place via a Raman transition [6]. The small signal gain profile according to the theory of Panock and Temkin [7] is shown in Fig. 1 for a D_2O pressure of 4 torr and a range of pump powers. In the case of a non-saturating pump (see for example the curve labeled $\alpha/\gamma=0.3$) it consists of two peaks of equal height, one on line center and the other offset from line center by an amount which corresponds to the offset of the pump frequency from the frequency of the absorbing transition. Provided that the cavity modes are sufficiently closely spaced so that there is at least one within each peak of the profile, it is reasonable to assume that at least two FIR modes develop, one under each peak.

In agreement with a range of theoretical papers [8, 9, 10, 11] we express field amplitudes in terms of their respective Rabi flipping frequencies.

for the pump $\alpha = \mu_{21} E_p / 2\hbar$

for the FIR $\beta = \mu_{23} E_{FIR} / 2\hbar$ (1)

where μ_{21} and μ_{23} are the dipole moments of the pump and FIR transitions respectively. The field amplitudes can be expressed in dimensionless units if α and β are divided by the collisional relaxation rate γ, assumed to be equal for all rotational levels involved. Values of α/γ, $\beta/\gamma \ll 1$ correspond to the small signal regime where frequency shifts due to the Stark effect, mode coupling and power broadening can be neglected. All these effects are noticeable for α/γ, $\beta/\gamma = 1$ and strong coupling and saturation are observed at α/γ, $\beta/\gamma \gg 1$.

The leading edge of the pump pulse is usually quite steep and saturating pump intensities are rapidly reached. With increasing α the small signal gain profile is modified as shown in Fig. 1. Due to the ac Stark effect, both gain profiles move outwards in frequency. The modes developed at the original positions of the peaks see a reduced gain, whereas spontaneously emitted radiation at frequencies shifted further away from line center experiences a considerably larger gain. The frequency of an established mode can only change via dispersion effects, but new modes can grow resulting in mode jumping, especially in a FIR laser where the gain coefficients are usually very high (approx. $1 cm^{-1}$). One would expect that the observed spectral distribution of the laser emission, assuming individual modes are not resolved, reproduces to a certain degree the outwards shifting gain profile. However, the gain profile is profoundly modified when the FIR intensity has reached a saturating level. This is illustrated in Fig. 2 where the pump intensity and the intensity of a FIR mode at the

Raman frequency grow together. The curves represent the gain profiles of a weak probe mode for the specified pump intensity and in the presence of the main FIR mode at the Raman frequency [12]. The shifting of the gain peak in the direction opposite to the line center, which is minor in this particular case, stops at a certain moment and is reversed.

Laser emission would be expected to start at the Raman frequency and then show a tendency, like the peak of the probe gain profile, to move outwards, in the direction opposite to the line center. Based on the same qualitative arguments one would then expect the emission to remain at a fixed frequency and later perhaps even move in the opposite direction. Our simplified picture is, of course, not self-consistent : as soon as the emission peak moves, our assumption of a fixed main mode at the Raman frequency is no longer correct. Similar behaviour with oppositely directed frequency shift and much smaller intensity would be expected for the line center emission, provided it is not completely suppressed by the presence of an intense Raman mode [8].

Mode interaction phenomena are very important in this context. They are responsible for the rapidly decreasing gain at line center (Fig. 2), as discussed in detail in [8]. While a theory to treat mode interaction in FIR lasers has been developed [10] and numerical codes exist to predict at least the interaction of a limited number of modes, a self-consistent simulation of the spectral profile of the laser emission developing under the influcence of a time- varying pump pulse is a formidable task which, to our knowledge, has never been attempted.

Mode interaction effects can further be complicated by the presence of other active transitions in the molecule, such as cascade and ground-state refill transitions. It has been shown [12] that a cascade line such as the 359μm line in D_2O, does not greatly affect the main transition, and a three-level theory is still adequate to describe the system. A refill transition in the ground state, however, could have an important effect by forming a coupled 4-level system of the V-Λ type [9], where the Raman oscillation in one transition enhances the line center oscillation in the other transition. In the case of the D_2O 385μm transition, however, the refill line at 239μm [5] is a weak line and hence of little importance.

The reader who is familiar with the theoretical treatment may have wondered why the gain peak at the Raman line (R) can shift in the direction of the line-center (LC) with increasing FIR power, as indicated in Fig. 2 (and in fact also observed in our experiment; see for example Fig. 8 and 9). Arguments based on the dressed atom approach [11] can readily give the resonance position of spectral features and for the case of a main FIR mode at the Raman frequency one obtains

$$\omega_{1,2} = -0.5\,\Delta \pm (\Delta^2/4 + \alpha^2 + \beta_0^2)^{1/2} \qquad (2)$$

$$\omega_3 = -\Delta \qquad (3)$$

where Δ is the difference between the pump frequency and the line center frequency of the absorbing transition. Equation (2) describes the outward shifting of both the LC and R lines with increasing α, the ordinary Stark effect. However, it also shows that a similar outward shift occurs due to increasing FIR power which seems to contradict the computed curves of Fig. 2. The explanation resides in the shape of

the resonance features of the gain profile given by the Eq. (2) and (3). At the frequencies given by Eq. (2) a simple peak is observed which can transform into a dip at high power. When either the pump or the FIR power grows, it moves further away from the line center. Equation (3), however, describes an asymetric feature as shown in Fig. 3 where the three resonance features are separated by assuming artificially small relaxation rates and hence narrow resonances. The positive part of the asymmetric (dispersion-like) feature is on the right, i.e. pointing towards line center. At pressures typical for the operation of a D_2O laser the two features are superimposed and appear as a peak that can also shift to the right on the frequency scale with increasing FIR power. It is difficult to find an intuitive picture to describe this effect.

In general, under the influence of multiple modes the gain profiles become very complex and numerical codes are required to study their behaviour.

3. EXPERIMENT

The study of the time resolved emission spectrum of our D_2O laser has been carried out using the experimental set-up shown in Fig. 4. The 4m long FIR laser resonator was folded by means of two wire grids into three sections. Two sections of roughly equal length were pumped by two CO2 laser beams. They were derived from a common oscillator and, after amplification to about 60J each, were coupled into the cavity via the grids. The third much shorter section remained unpumped. The stable cavity was formed by a concave mirror and the

plane surface of a TPX lens which acts as the output coupler. The D_2O laser produced 1μs long pulses of up to 200mJ usually consisting of two to three longitudinal modes. The existence of several modes is concluded from the deeply modulated pulse shape at the intermode frequency, as seen on a fast detector, and from the observed width of the emission profile. The system was operated in its standard set-up for Thomson scattering but with a metal ball at the intersection of incident and scattered beam inside the tokamak and strong attenuation in front of the detection system. This part of the beam path is not shown in the figure. It is likely that the unsatisfactory shot to shot reproducibility was to a large degree due to this set-up which is sensitive to small mechanical vibrations of the metal ball support.

The laser emission was mixed in a quasi-optical diplexer with the output of a CW optically pumped CD_3Cl laser and detected by a Schottky-barrier diode operating in heterodyne mode. Signal analysis was performed at the intermediate frequency by seven coaxial waveguide filters, with a bandwidth of 80MHz each. Four channels were centered around the Raman frequency and three around the line center frequency. The signal from each channel was digitized at a sampling rate of 32MHz by LeCroy model TR8837 CAMAC units with 8 bit resolution. Digital oscilloscopes were used to record the pulse shapes of the CO_2 pump laser and the D_2O FIR laser. For numerical analysis all data were transfered to a PDP-11 computer.

At each D_2O gas pressure of interest a series of typically ten laser shots was fired. The raw data show the time evolution of the FIR power for each frequency channel. A separate calibration of the total gain of each channel by means of a black body source allowed scaling

of the signals so that spectral profiles could be obtained at 31ns time intervals. Clearly the spectral resolution of 80MHz was insufficient to resolve individual longitudinal modes which were separated by 40MHz. Hence mode competition effects could not be directly observed. Since the recording system used to monitor the FIR pulse shape was not fast enough to clearly resolve the beat signal due to the presence of several modes, single mode and multimode operation could not be distinguished. Only shifts of the total emission envelope could thus be observed.

4. RESULTS AND DISCUSSION

For narrow band FIR emission single mode pumping is essential. It has been shown [10] that two pump modes create multiple FIR gain peaks separated from each other by the intermode spacing and not just two peaks at the corresponding Raman frequencies. This is due to nonlinear effects resulting from the induced beating of the population densities. Hence one would expect broad band emission in the FIR as soon as the pump beam is multimode. This is indeed observed. In Fig. 5 we show the recorded signals of 7 channels for two consecutive shots. On the left hand side the pump pulse (top graph) was single mode, whereas on the right hand side the modulation of the pulse indicates multimode operation (beat signal not resolved).

Each channel was 80MHz wide and is labeled by the offset of its center frequency from the Raman frequency. While the three channels around the line center, namely 400, 320 and 240MHz, quite clearly show a signal on the right hand side (multimode pumping) there is, apart

from an initial spike, practically no signal in the single-mode pump case. The presence of the spike indicates that a mode on or near line center starts to develop, but is rapidly and efficiently suppressed by the Raman mode, as has been discussed in ref [8]. Also, for multimode pumping, the emission around the Raman frequency shows a larger spectral spread.

Due to the weak signal in the vicinity of the line center and the restricted dynamic range of our recording system, interpretation of LC data was difficult. We will therefore from now on restrict our discussion to the behaviour near the Raman line.

Figure 6 shows a series of curves representing the D_2O laser emission as recorded by 4 spectral channels covering a band of 320MHz around the Raman line. Each curve corresponds to a particular instantaneous pump power and represents an average over 10 shots. The curves are arranged to form a 3D-plot. Before averaging, the FIR signal for each shot was first represented as function of pump power, instead of time, resorting to linear interpolation in order to get a fixed discretization. This procedure avoids the problems arising from the jitter in the onset of the laser pulses with respect to a fixed time marker. The 30 curves of Fig. 6 refer to the falling part of the CO_2 pulse and to a pressure of 3.5 torr. The emission maximum occurs quite clearly at the Raman frequency for weak pump intensities and is shifted outwards by a full channel width at maximum pump power, a clear indication of the pump induced AC Stark effect. This is not usually observed in similar experiments [13, 14], probably because of inadequate time resolution. The behaviour is similar during the rising part of the CO_2 pulse. However, the maximum frequency shift is smaller

in this case. It seems that the short rise time (300ns) of the CO_2 pulse is insufficient for the buildup of new modes at a shifted frequency, whereas this does take place during the 1μs long tail of the pump pulse.

A similar picture showing a frequency shift of 1 channel width in the opposite direction has also been obtained for the channels around the line center frequency. The set of data, however, does not lend itself to a 3D representation similar to Fig. 6 because of the much weaker signals due to the suppression mechanism mentioned above, resulting in large fluctuations.

In Fig. 7 we again show data for 12 averaged shots and for a pressure of 1 torr. This time the FIR power is plotted as function of frequency and time. Again, FIR emission starts at the Raman frequency where a local maximum is rapidly reached (peak 1), earlier than the peak of the pump pulse occurring at the time of 280ns. Even with the limited resolution, the frequency shift towards a new maximum (peak 2) at an offset of -80MHz and at a time of 770ns is clearly visible. Later, at decreasing pump power, the FIR frequency of maximum emission shifts back towards the Raman frequency. A third local maximum (peak 3) is reached late in the pump pulse, at 1.4μs. The emission spectrum is noticeably narrower during this part where the pump power is fairly constant. Obviously rapid variations in pump power are not favourable for a stable and narrow emission profile. Flat-topped pump pulses would probably give much better results.

The spectral shift of the laser emission during the pump pulse has been analyzed in more detail. Whereas the frequency of the maximum

is easily determined, (even with the limited resolution of 80MHz determined by the receiver channels), an estimate of the half width of the profile requires interpolation.

Assuming a smooth emission profile that comprises several cavity modes (spaced at 40MHz) it is reasonable to use a spline fit to the discrete data points. In this way the frequency shift can be displayed as a continuous curve rather than as a sequence of jumps by ± 80MHz. An example for this kind of analysis is given in Fig. 8 representing data of 10 shots at a pressure of 4 torr. The position in frequency of the maximum intensity as well as the half maximum intensity points on either side are shown as function of pump power. Only the time interval during the falling part of the pump pulse has been considered. The Stark shift due to increasing pump power is again clearly visible and a slight broadening of the emission profile is also observed. The inversion in the slope of the frequency shift at the highest pump powers can obviously not be explained by the Stark effect alone. However, as discussed in Chapter 2, a shift towards line center is expected at high FIR power levels.

With the method described above we have displayed the positions of the half-intensity points on either side of the peak for all recorded data. The FWHM is approximately 150MHz and thus encompasses typically 4 resonator modes. Although in fact very little pressure broadening of the emission spectrum has been observed it seems that the distribution is slightly broader at higher pressures in qualitative agreement with theory. There is some indication that the low level contribution is more strongly pressure dependent, in agreement with the observations of Woskoboinikow [15].

Figure 9 shows the major results summarized in three curves for each D_2O pressure investigated. On the left hand side the FIR power integrated over all spectral channels is shown as function of pump power during the full pulse duration. In this representation we obtain curves that show a hysteresis-type behaviour. Certain points, equidistantly spaced in time, are marked for comparison with the middle and right hand side diagrams. These show the frequency and power of the emission maximum as function of time, as obtained from a spline fit to the measured spectral data points, as discussed earlier. The analysis of these diagrams reveals the following facts :

When we follow the time evolution of the FIR power on Fig. 9a (going round the curves in the sense of increasing numbers of the time markers) we note a distinct pressure dependent behaviour. At low pressure the FIR power increases steeply as function of pump power before it levels off, indicating a saturation effect. During the time interval of decreasing pump power the FIR emission is considerably lower. The situation is reversed at high D_2O pressure (8 Torr). Only at the intermediate pressure of 4 torr (which yields maximum FIR energy output per pulse) the FIR power follows almost linearly the pump power.

At low pressure the Stark effect appears to be quite important. At 0.5 torr the FIR radiation develops at a frequency which is shifted by 80MHz from the Raman line center and stays there. It seems to move inwards towards the Raman frequency only towards the end of the pump pulse. However, at this stage the FIR power is very low and hence the data uncertain. For this reason this part of the trace is not shown in the figure. The FIR grows very rapidly into a saturated region where

it remains up to the peak of the CO_2 laser pulse. It then decays almost proportionally with the pump.

At 1 torr the FIR power still grows rapidly and shows signs of saturation. The emission peak is initially at the Raman frequeny and moves outwards to reach a maximum shift at the time when the CO_2 laser power has returned to one quarter maximum, but the FIR laser power is still about half its maximum. After this point the frequency rapidly returns to the Raman frequency and a secondary power peak develops (see Fig. 8c).Hence a doubly peaked FIR pulse is observed whereby the two peaks occur at roughly the same frequencies.

This double peaked structure is also observed at 4 torr and again the two peaks occur at similar frequencies, while the time of the intervening trough coincides with the time of maximum frequency shift. During the first 400ns the pump and FIR powers grow and decay almost in proportion to each other.

At high pressure (8 torr) two peaks are still observed, this time with slightly different frequencies; the second one is displaced inwards, towards the line center. The FIR power remains at a high level for an extended time. Hence FIR pulses with a long, reasonably flat top can be obtained under these conditions.

At 8 torr we also note that the frequency remains fairly constant, at least up to the second maximum. Later a frequency shift towards the line center position is observed. This is only the case at 8 torr, whereas for all lower pressures a shift in the opposite direction is observed.

A superficial comparison of the diagrams in Fig. 9b might suggest that the frequency stability is best at 0.5 torr. However, the following points have to be taken into account :

(1) The early part of the build-up phase during which the emission shifts from the Raman frequency to -60MHz is not shown on the graph.

(2) A frequency shift of 35MHz occurs during the first 400ns and therefore during the interval that contains the major part of the pulse energy.

(3) The channels of our receiver system could only cover the frequency range down to -160MHz from the Raman frequency. Already for shifts of the emission profile beyond -80MHz the interpolation procedure is no longer reliable. This may cast some doubts on the apparent frequency stability during the end of the pulse as shown in Fig. 9b.

The double-humped FIR pulse shape mentioned above is an interesting feature and we present some further observations in Fig. 10. This time the evolution of the FIR intensity in the Raman channel is displayed rather than the intensity of the spectral peak which varies in frequency. Again we clearly observe two peaks, one slightly before the peak of the pump, the other later. The separation of the peaks is quite clearly pressure dependent. This is a systematic effect but so far without obvious explanation. We will discuss it in some more detail in the next section.

5. ANALYSIS

The influence of mode competition in suppressing line center oscillation and also the influence of the Stark effect have been discussed earlier and in several previous publications [8, 9, 10, 11] and will not be further discussed here. Instead we will put forward some arguments to explain why a stable frequency is only obtained at high pressures. Our arguments and numerical results are based on the work described in [11]. The numerical code described in this reference allows computation of the gain profile of a weak FIR probe mode in the presence of an arbitrarily intense main FIR mode. It is ideally suited to predict the tendency of a neighbouring mode to grow in the presence of a developed main mode, but it cannot, in this form, describe the growth, the overtaking and eventual suppression of the initial mode by the new mode.

In the code field amplitudes are expressed as dimensionless quantities α/γ for the pump and β/γ for the FIR according to Eq. (1) and (2). Based on the measured FIR power density of 8kW/cm^2 and the published value [3] for the dipole moment and relaxation time constant we calculated a β/γ value of 15 at 4 torr, indicating very strong saturation. Our experimental results (e.g. the amount of the Stark shift) indicate that this is probably about a factor of 3 to 5 too high. We have no really convincing explanation for this discrepancy, but note that in other experiments [4, 16, 17, 18] a similar disagreement has been observed.

For an α/γ of 1, hence just approaching saturation, we present in Fig. 11 the conditions representative of our experiment at a pressure of 4 torr. As function of the field strength β/γ of the main FIR mode at the Raman frequency, we show its gain as well as the gain of modes separated from the Ramain mode by ±40 and ±80MHz. (Note that 40MHz is the cavity mode spacing and that the line center is at +320MHz; hence Stark shifted frequencies have negative values.) In the gain profiles the effect of the main FIR mode at the Raman line has been included. As a consequence, the gain at the outwards shifted frequencies is suppressed for a field strength of the main mode greater than 1.6. Since the gain is highest for the main mode (Raman mode), stable operation is expected in this case for all FIR intensities.

When the field strength of the pump is doubled the conditions shown in Fig. 12 are obtained. For low FIR power the gain at Stark shifted frequencies is higher and mode jumping may well occur. However, if the intensity of the main mode grows rapidly into the region where it has the highest gain there may be insufficient time for the buildup of a new mode and the situation will be stable.

We will now consider a low pressure case. Here the gain profiles are narrower and a given IR or FIR intensity corresponds to higher α or β values. At $\alpha/\gamma=4$ (which corresponds to the same pump intensity as $\alpha/\gamma=1$ at 4 torr) we see (Fig. 13) that the situation is still stable, but the gain at the neighbouring resonator mode, 40MHz further out is fairly large. At $\alpha/\gamma=8$ (Fig. 14) mode jumping quite clearly can be expected. Our experimental results indicate indeed a stronger tendency for frequency shifting at lower pressures. On the other hand, we noticed in connection with the double-hump structure a faster reaction to

changing conditions at high pressures. This is consistent with the observation that the FIR gain is unsaturated at high pressures and new modes at shifted frequencies can build up more rapidly than in the heavily saturated low pressure case.

The bottleneck effect [19] is also more important under saturated conditions. It effectively reduces the supply of molecules which can be pumped, since they are only available again after a time delay given by the vibrational relaxation time. This reduces the pumping efficiency and slows down the reaction time of the system and therefore might also partly be responsible for the pressure dependent separation in time of the two peaks.

In addition to the arguments outlined above, frequency shifts and the structure of FIR pulse shapes also might be influenced by the slow response time of the FIR laser output to changes in pump power. In the 4m long resonator the round-trip time which is representative of the time to react to external changes is 27ns. However, since it is difficult to assign univocally an observed effect to a presumed cause, we will not pursue our discussion of this point.

From some simple arguments we have found a possible explanation for our experimental results. However, the dynamic behaviour of an optically pumped FIR laser is extremely complex and a theoretical simulation that includes all parameters of a given experiment is not feasible.

6. CONCLUSIONS

Frequency- and time- resolved investigations of an optically pumped FIR laser have produced several interesting results. Theoretical considerations based on a simplified physical picture, have allowed us to explain, at least qualitatively, certain observed effects. Several others are not, at present, well understood.

Stable operation of the laser on a spectrally narrow pulse involves the following considerations : high pressure operation is required for frequency stability. The pressure broadening is not significant enough to impose a strict limit, but a compromise has to be found if high output power is required in addition to a stable frequency and narrow band width. In our system maximum output power is achieved around 4 torr. Rapid variations of the pump power are undesirable and could be avoided by flat-topped pump pulse shapes, which are, however, not easy to produce.

The pump induced Stark effect has clearly been demonstrated. However, the FIR power can also shift the frequency; in fact for certain combinations of the two effects a shift in the opposite direction to the Stark shift can be obtained.

A much weaker emission has occasionally been observed at the line center frequency. It is rapidly and efficiently suppressed by mode interaction effects, except in the case of a multimode pump. If observable, the line center emission also manifests a Stark shift in the direction opposite to the Stark shift of the Raman frequency.

Saturation effects are observed at low, but not at high pressure.

A double-humped, pressure dependent temporal pulse shape is observed. Except at 8 torr the trough between the pulses seems to occur at the time of maximum frequency shift and thus is probably linked to the buildup of new modes at new, shifted frequencies.

Almost negligible pressure dependence of the emission profile has been observed, except perhaps for the low-level background radiation which seems indeed broader at higher pressures.

Repetition of these investigations with a detection system which allows resolution of individual modes (resolution of 10-20MHz) could be extremely valuable. Much of what remains at present somewhat speculative could then probably be explained.

Acknowledgement - This work was partly supported by the Fonds National Suisse de la Recherche Scientifique.

REFERENCES

[1] A. Semet, L.C. Johnson, D.K. Mansfield, "A high energy D_2O submillimeter laser for plasma diagnostics", Int. J. of Infrared and Millimeter Waves 4(2), 231 - 246 (1983).

[2] P.D. Morgan, M.R. Green, M.R. Siegrist, R.L. Watterson, "The development of far-infrared lasers for Thomson-scattering measurements on tokamak plasmas", Comments Plasma Phys. & Contr. Fus. 5(4), 141 - 158 (1979)

[3] T.A. DeTemple, "Pulsed optically pumped far infrared lasers", Infrared and Millimeter Waves, 1, ed. K.J. Button, New-York, 129 - 184 (Academic 1979).

[4] R. Behn, I. Kjelberg, P.D. Morgan, T. Okada, M.R. Siegrist, "A high power D_2O laser optimized for microsecond pulse duration", J. Appl. Phys. 54(6), 2995 - 3002 (1983).

[5] P. Woskoboinikow, H.C. Praddaude, W.J. Mulligan, D.R. Cohn, B. Lax, "High-power tunable 385μm D_2O vapor laser optically pumped with a single-mode tunable CO_2 laser", J. Appl. Phys. 50(2), 1125 - 1127 (1979).

[6] T.Y. Chang, J.D. McGee, "Off-resonant infrared laser action in NH_3 and C_2H_4 without population inversion", Appl. Phys. Lett. 29(11), 725 - 727 (1976).

[7] R.L. Panock, R.J. Temkin, "Interaction of two laser fields with a three-level molecular system", J. of Quantum Electron. QE-13(6), 425 - 434 (1977).

[8] M.A. Dupertuis, M.R. Siegrist, R.R.E. Salomaa, "Competition between Raman and line-center oscillations in optically pumped far-infrared lasers", Phys. Rev. A, 30(5), 2824 - 2826 (1984).

[9] M.A. Dupertuis, R.R.E. Salomaa, M.R. Siegrist, "Raman and line centre oscillation selection in coherently pumped four-level FIR lasers", Opt. Com. 54(1), 27 - 32 (1985).

[10] M.A. Dupertuis, R.R.E. Salomaa, M.R. Siegrist, "Two-mode optical pumping of a laser", IEEE J. Quant. Electron. QE-20(4), 440 - 449 (1984).

[11] M.A. Dupertuis, M.R. Siegrist, R.R.E. Salomaa, "Stability of single-mode, optically-pumped lasers", to be published in IEEE J. Quantum Electron.

[12] M.A. Dupertuis, M.R. Siegrist, R.R.E. Salomaa, "Line selection in off-resonantly pumped multi-level systems", to be published in Phys. Rev. A.

[13] B.G. Danly, S.G. Evangelides, R.J. Temkin, B. Lax, "Frequency tuning and efficiency enhancement of high-power far-infrared lasers", Infrared and Millimeter Waves 12, ed. K.J. Button, New-York, 195 - 278 (Academic 1984).

[14] J.R. Izatt, B.K. Deka, W. Zhu, "Simultaneous tunable Raman and fixed frequency oscillation of a CH_3F FIR laser", IEEE J. Quantum Electron. QE-23(1), 117 - 122 (1987).

[15] P. Woskoboinikow, W.J. Mulligan, R. Erickson, "385 μm D_2O laser linewidth measurements to -60dB", IEEE J. Quantum Electron. QE-19(1), 4 - 7 (1983).

[16] B.G. Danly, R.J. Temkin, "Dispersion in a laser-pumped molecular laser", IEEE J. Quant. Electron. QE-16(6), 587 - 589 (1980).

[17] Z. Drozdowicz, R.J. Temkin, B. Lax, "Laser pumped molecular lasers - Part I : Theory", IEEE J. of Quantum Electron. QE-15(3), 170 - 178 (1979).

[18] Z. Drozdowicz, R.J. Temkin, B. Lax, "Laser pumped molecular lasers - Part II : Submillimeter laser experiments", IEEE J. Quantum Electron. QE-15(9), 865 - 869 (1979).

[19] R. Behn, M.A. Dupertuis, I. Kjelberg, P.A. Krug, S.A. Salito, M.R. Siegrist, "Buffer gases to increase the efficiency of an optically pumped far infrared D_2O laser", IEEE J. Quantum Electron. QE-21(8), 1278 - 1285 (1985).

FIGURE CAPTIONS

Fig. 1 : Small-signal gain profiles for five different pump field amplitudes and a pump frequency offset $\Delta/\gamma=4$.

Fig. 2 : Small-signal gain profiles in the presence of a main FIR mode at the Raman frequency. The dimensionless amplitudes of the pump and the main FIR mode vary together. ($\Delta/\gamma = 4$).

Fig. 3 : Two small-signal gain profiles near the Raman line at very low pressure in the presence of a main FIR mode at Raman frequency. The position of the peaks is obtained as solution of Eq. 2 (with a symmetric peak near line center). Note the rapid transition from a positive to a negative peak as function of β_0. The position of the asymmetric peak at the Raman frequency is the solution of Eq. 3.

Fig. 4 : Configuration of the experimental system : LO = CO_2 laser oscillator; PA = TEA CO_2 preamplifier; LA = TEA CO_2 laser amplifiers; FIRL = D_2O FIR laser; HDS = heterodyne detection system. Individual components : LP = low pressure module; TM = TEA module; G = grating, OC1 = ZnSe output coupler; GA = SF_6 gas absorption cells; BS = beam splitter; WG = wire grids, OC2 = TPX output coupler; ST = scattering target; LOLB = local oscillator laser beam; D = diplexer; SDM = Schottky diode mixer; A = amplifier; FB = filter bank.

Fig. 5 : The signals recorded in each channel (correctly scaled) for two shots : the pump pulse was single mode on the LHS and multi-mode on the RHS. (Note that for clarity negative signals are not shown. The small spikes close to the base line at 320MHz in Fig. 5a, for example, are within the noise level, with a similar amount of negative going spikes.)

Fig. 6 : Averaged spectra of ten shots at a D_2O pressure of 3.5 torr, presented as function of pump power, for the falling part of the pump pulse only.

Fig. 7 : FIR emission as function of frequency and time. (Average of twelve shots at a pressure of 1 torr).

Fig. 8 : The frequency shift of the FIR emission maximum and the half-maximum points on either side, as function of pump power obtained from a spline fit of the averaged data of the ten shots at a D_2O pressure of 4 torr.

Fig. 9 : Spectrally integrated FIR power vs pump power, and frequency and power of the FIR peak as function of time for four different D_2O pressures. The time evolution is marked with numbered points (9a) which are also indicated along the time axes (9b, c).

Fig. 10 : FIR signal in the Raman channel for four different pressures, showing two peaks with a pressure dependent separation.

Fig. 11 : Small signal gain at five different frequencies around the Raman frequency, as function of the amplitude of a main FIR mode at the Raman frequency and for weak pumping. The D_2O pressure is 4 torr.

Fig. 12 : As Fig. 11, but for a stronger pump.

Fig. 13 : As Fig. 11 for a D_2O pressure of 1 torr. (Note that α/γ is adjusted to keep the pump power the same).

Fig. 14 : As Fig. 13, but for a stronger pump.

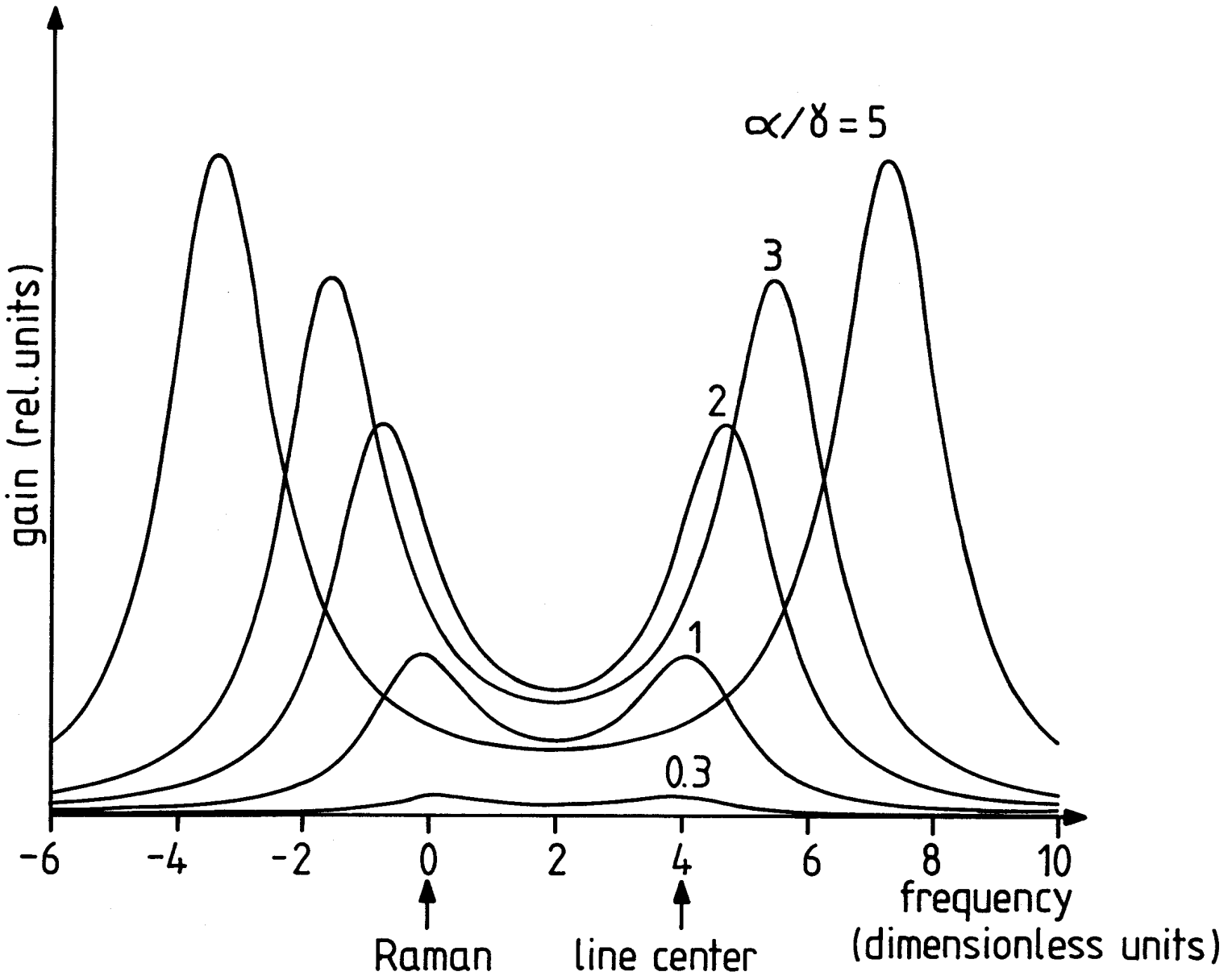
α/γ = 5
3
2
1
0.3
gain (rel.units)
-6
-4
-2
0
2
4
6
8
10
frequency
(dimensionless units)
Raman
line center

Fig. 1

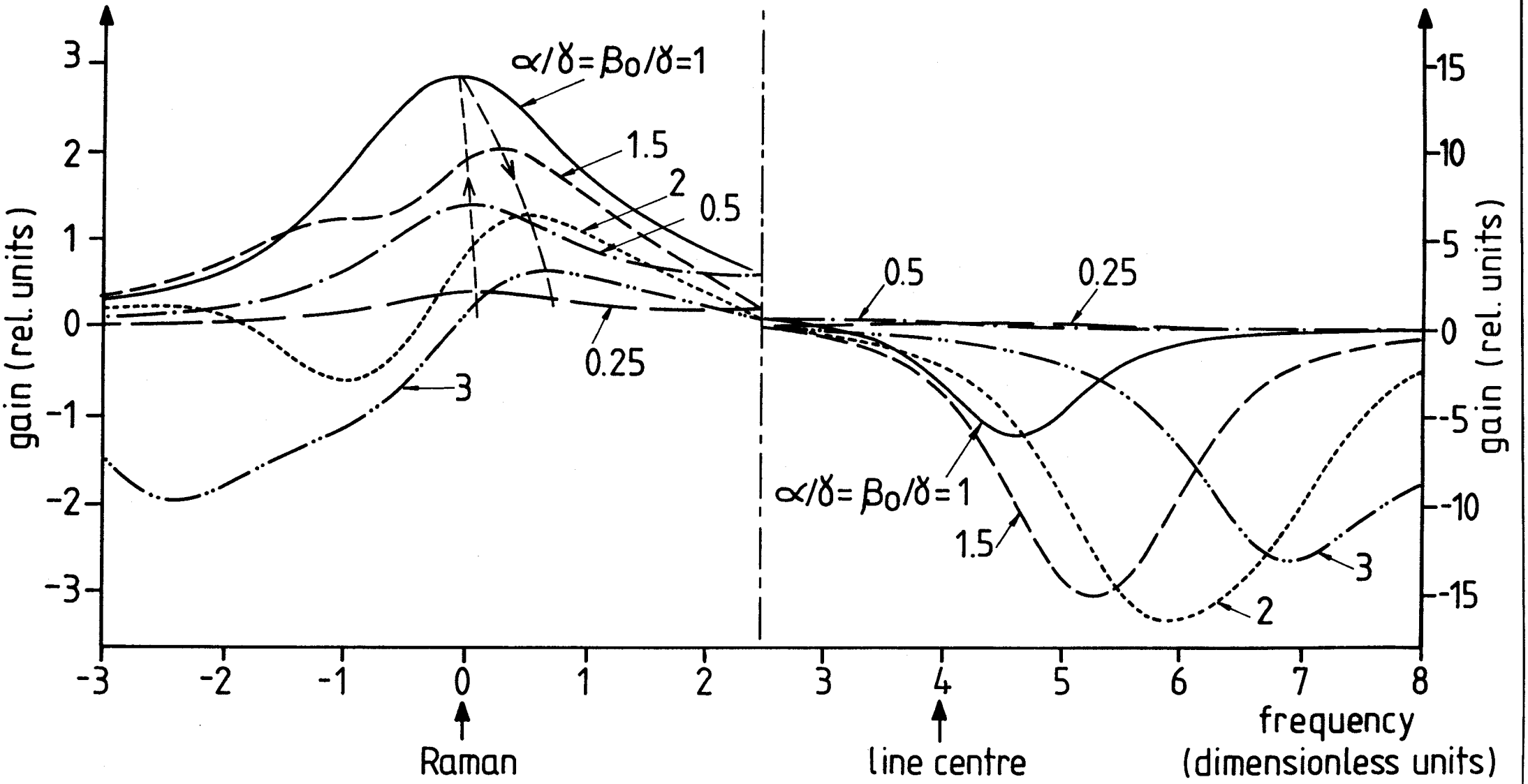
α/γ = β0/γ = 1
1.5
2
0.5
0.25
3
gain (rel. units)
Raman
line centre
frequency
(dimensionless units)

Fig. 2

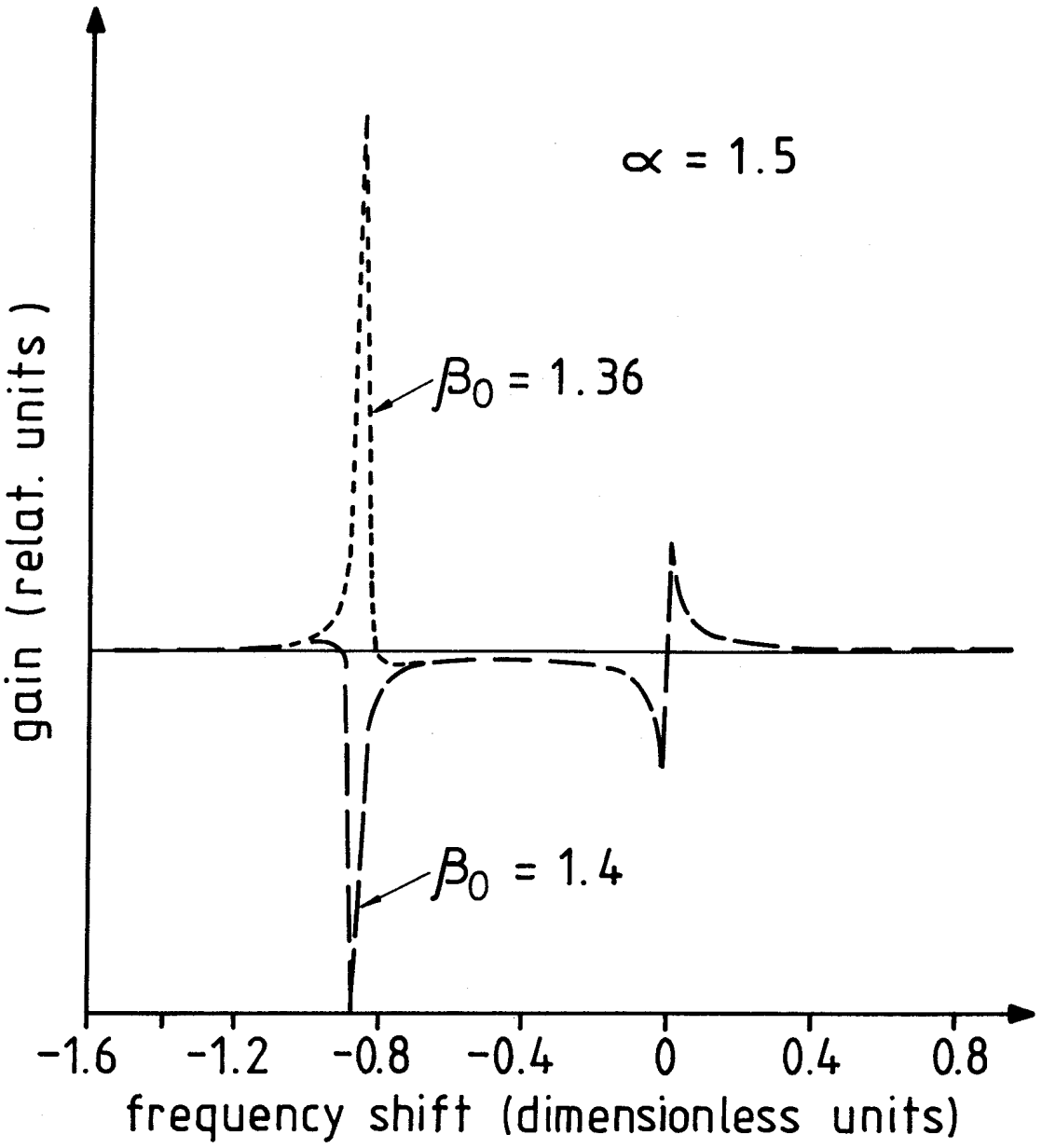
α = 1.5
β_0 = 1.36
β_0 = 1.4
gain (relat. units)
-1.6
-1.2
-0.8
-0.4
0
0.4
0.8
frequency shift (dimensionless units)

Fig. 3

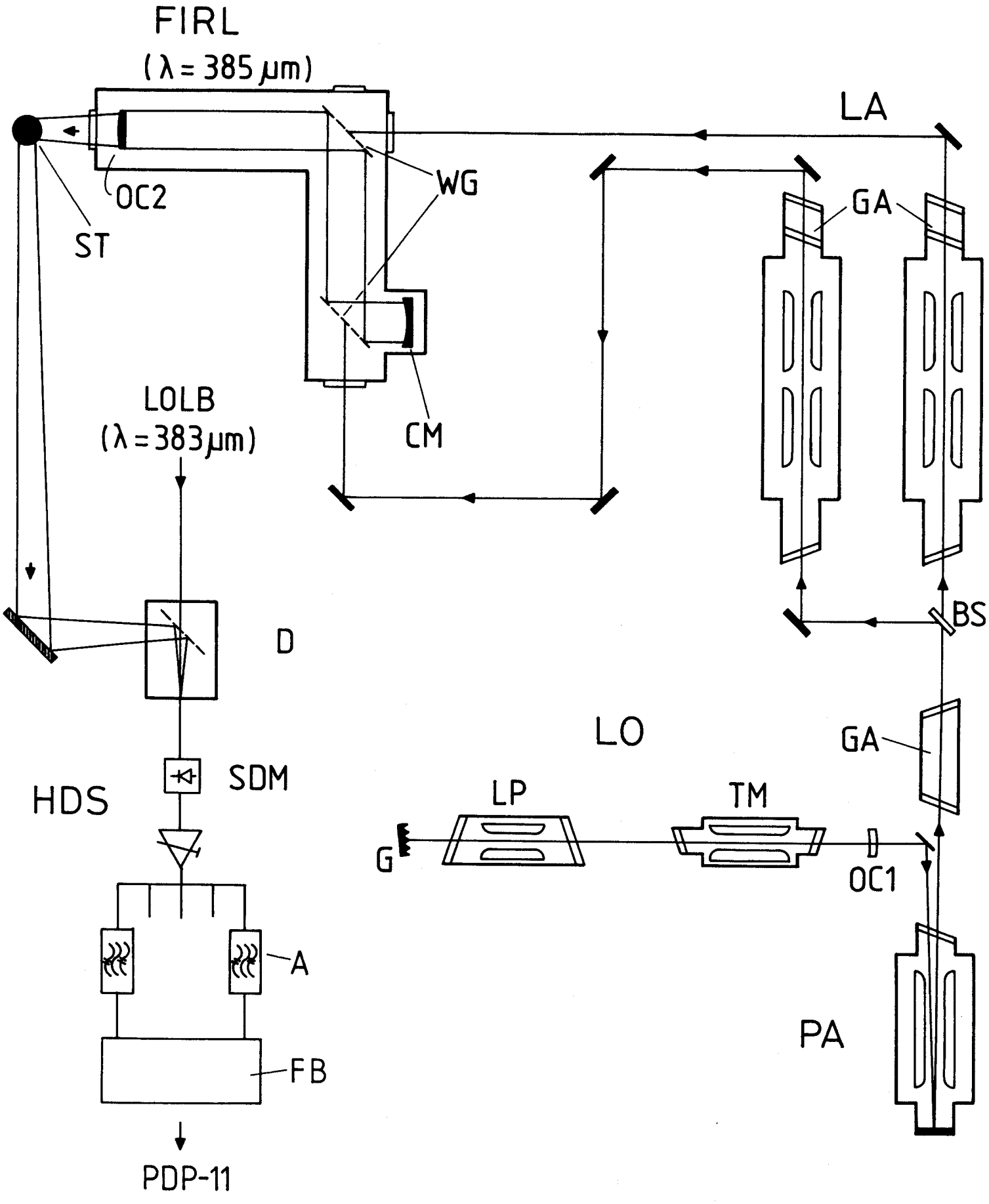
FIRL
(λ = 385 μm)
LA
OC2
WG
GA
ST
LOLB
(λ = 383 μm)
CM
BS
D
LO
GA
HDS
SDM
LP
TM
G
OC1
A
PA
FB
PDP-11

Fig. 4

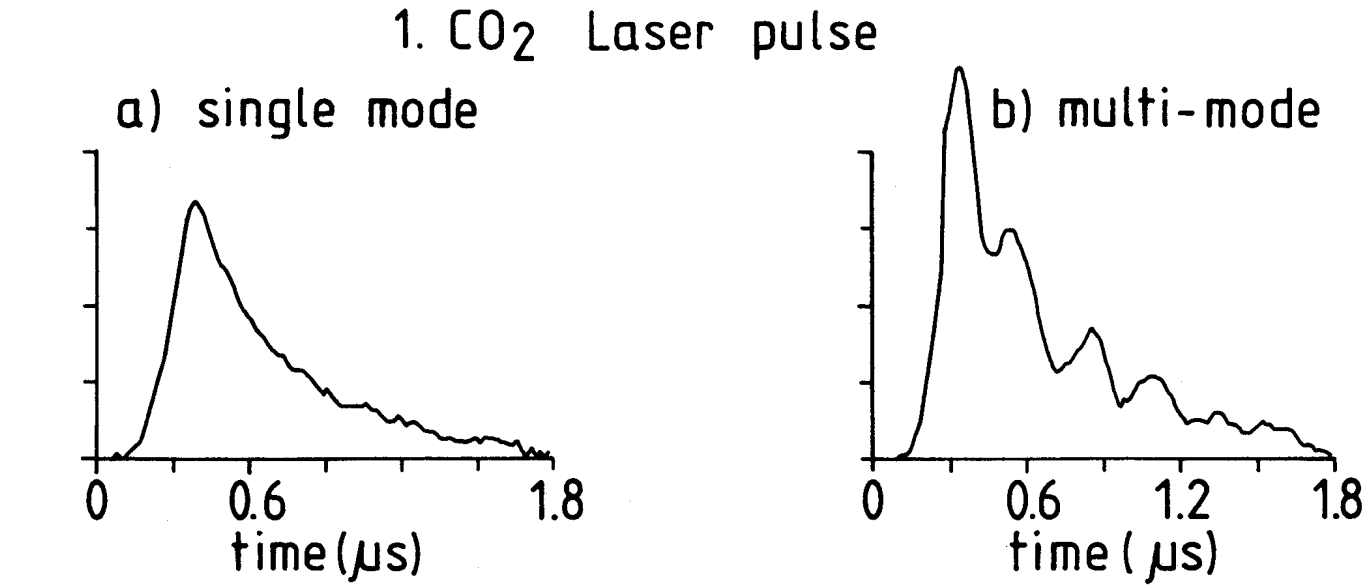
1. CO_2 Laser pulse
a) single mode
b) multi-mode
0
0.6
1.8
time (μs)
0
0.6
1.2
1.8
time (μs)

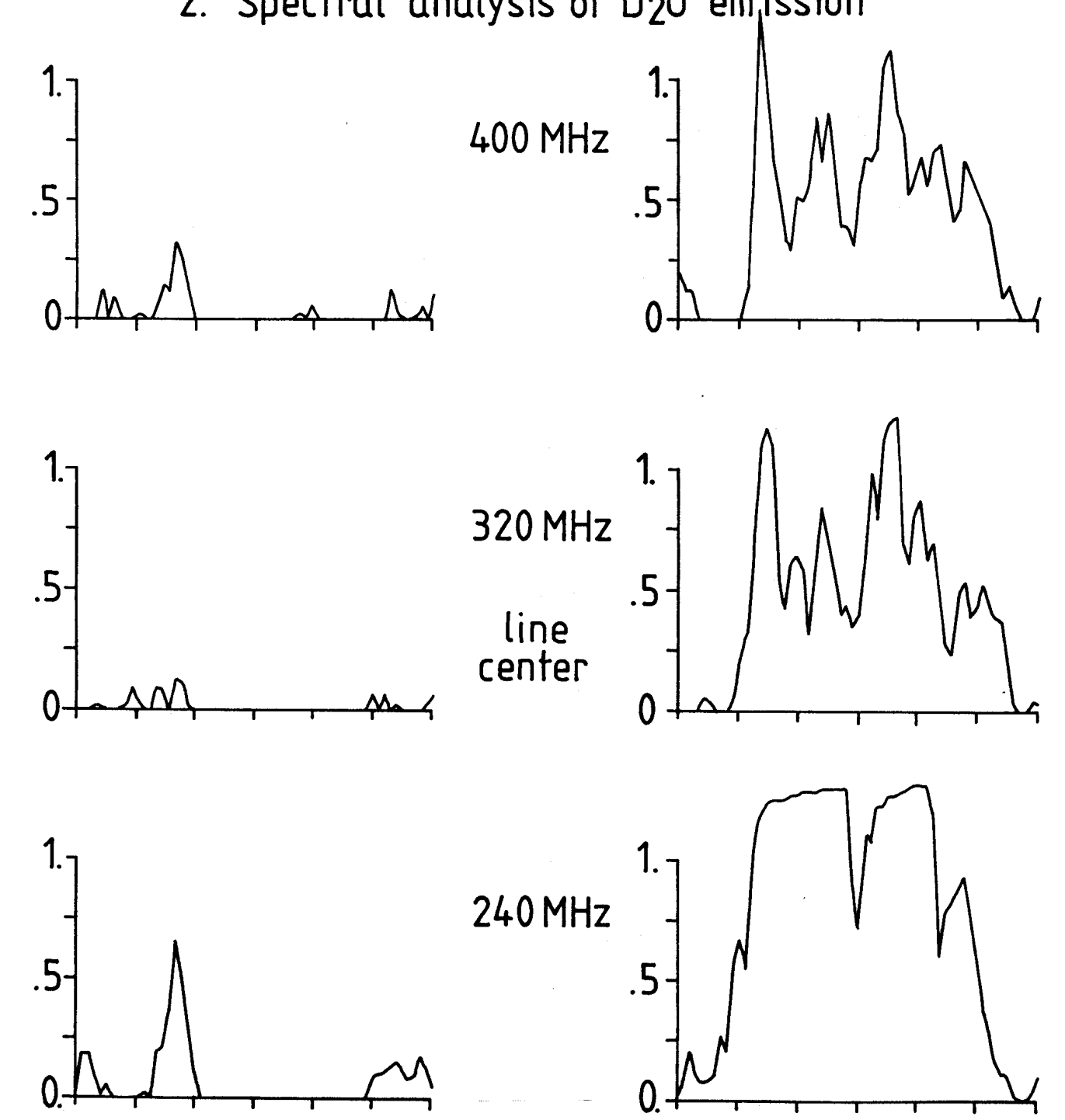
2. Spectral analysis of D_2O emission
1.
.5
0
400 MHz
320 MHz
line center
240 MHz

Fig. 5 a

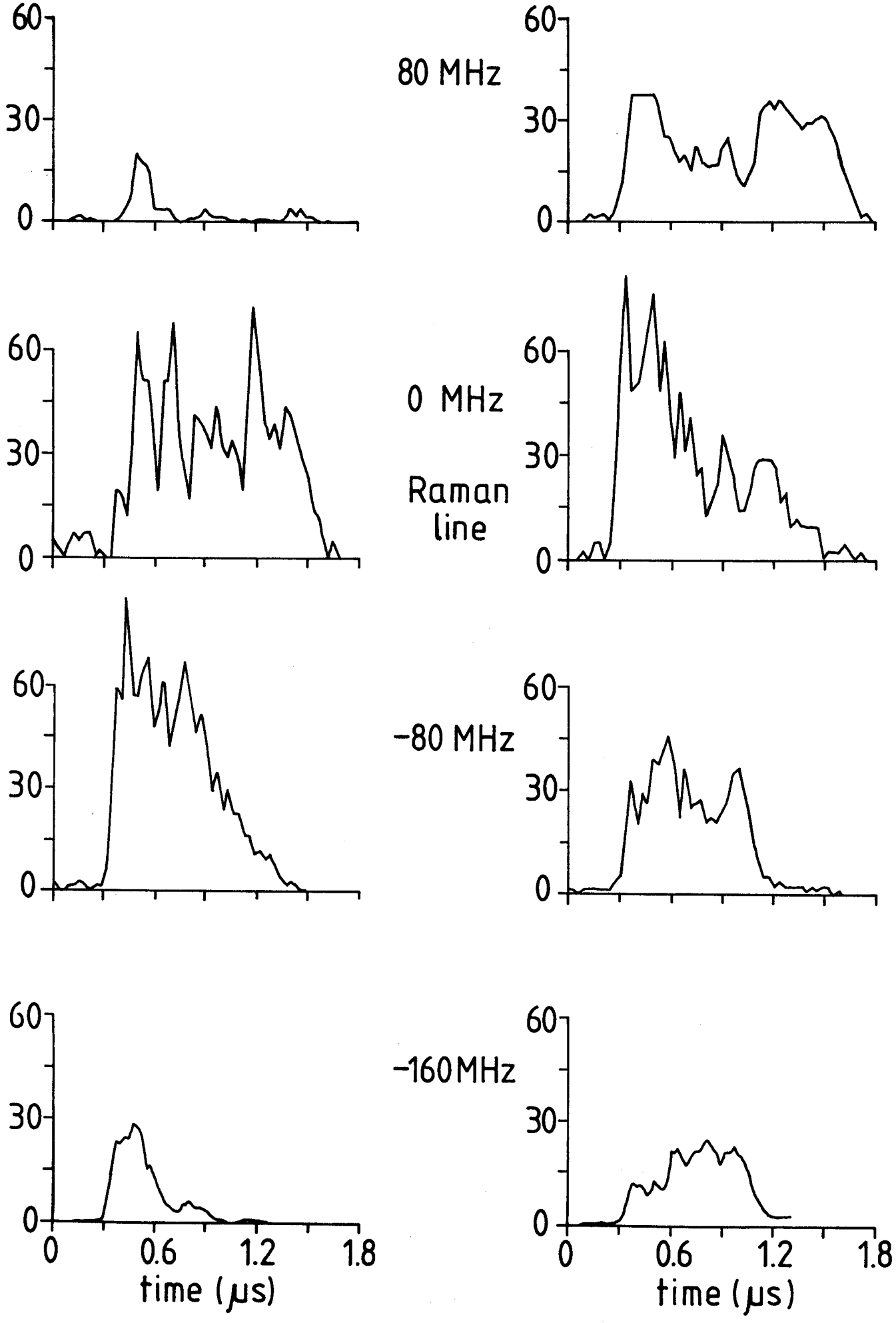

Fig. 5b

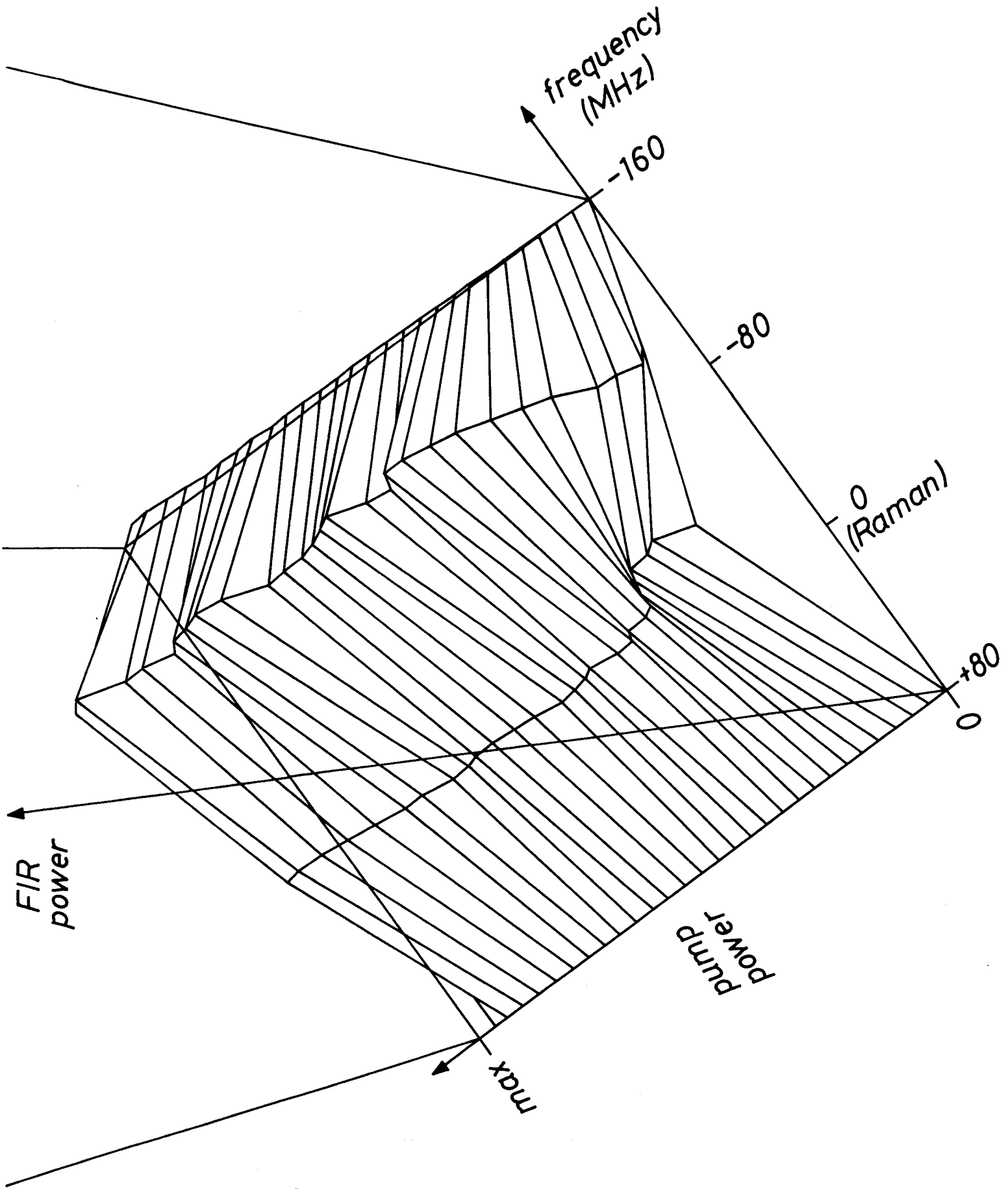

Fig. 6

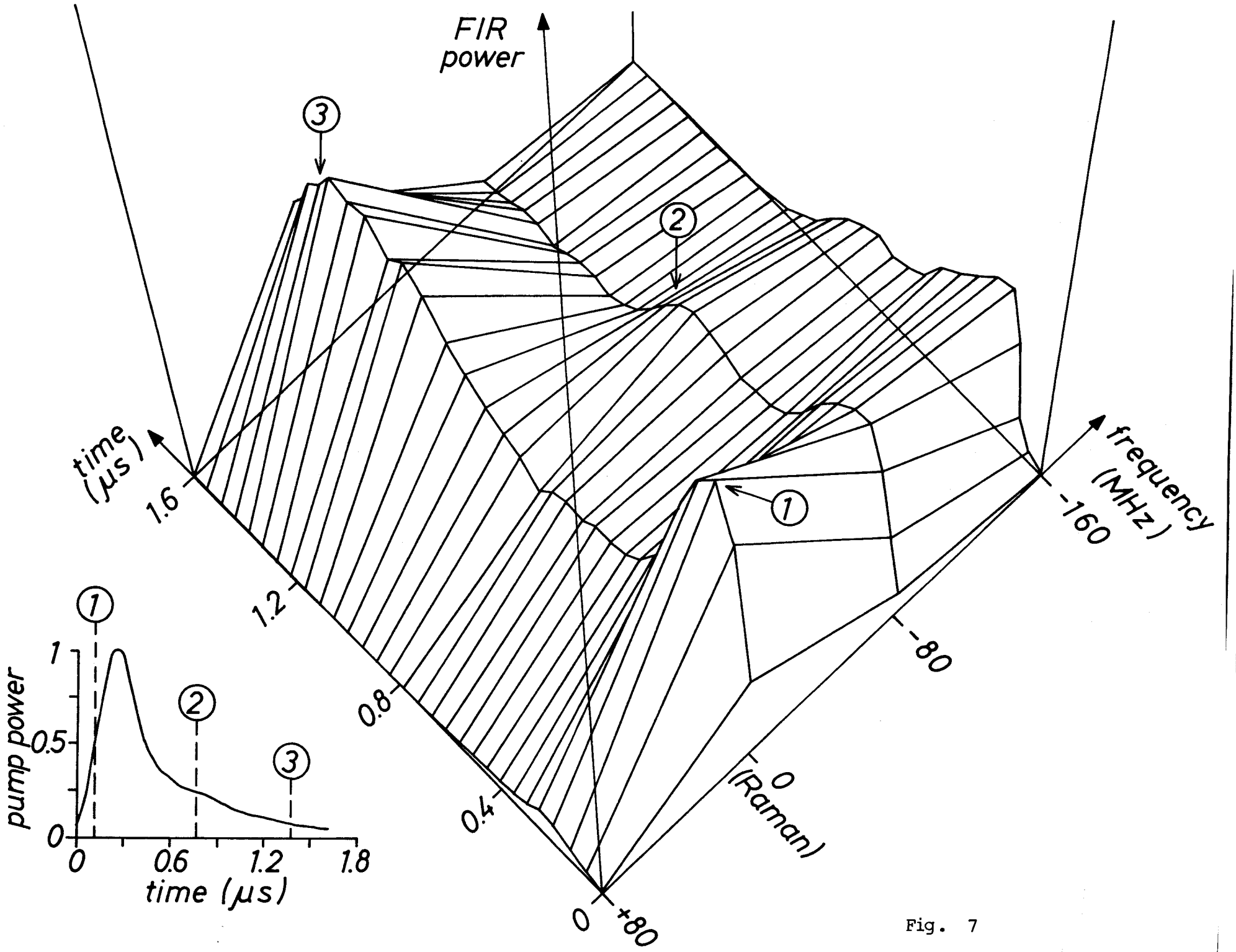
FIR
power
3
2
1
time
(μs)
1.6
1.2
0.8
0.4
0
+80
-80
-160
frequency
(MHz)
0
(Raman)
pump power
1
0.5
0
0
0.6
1.2
1.8
time (μs)

Fig. 7

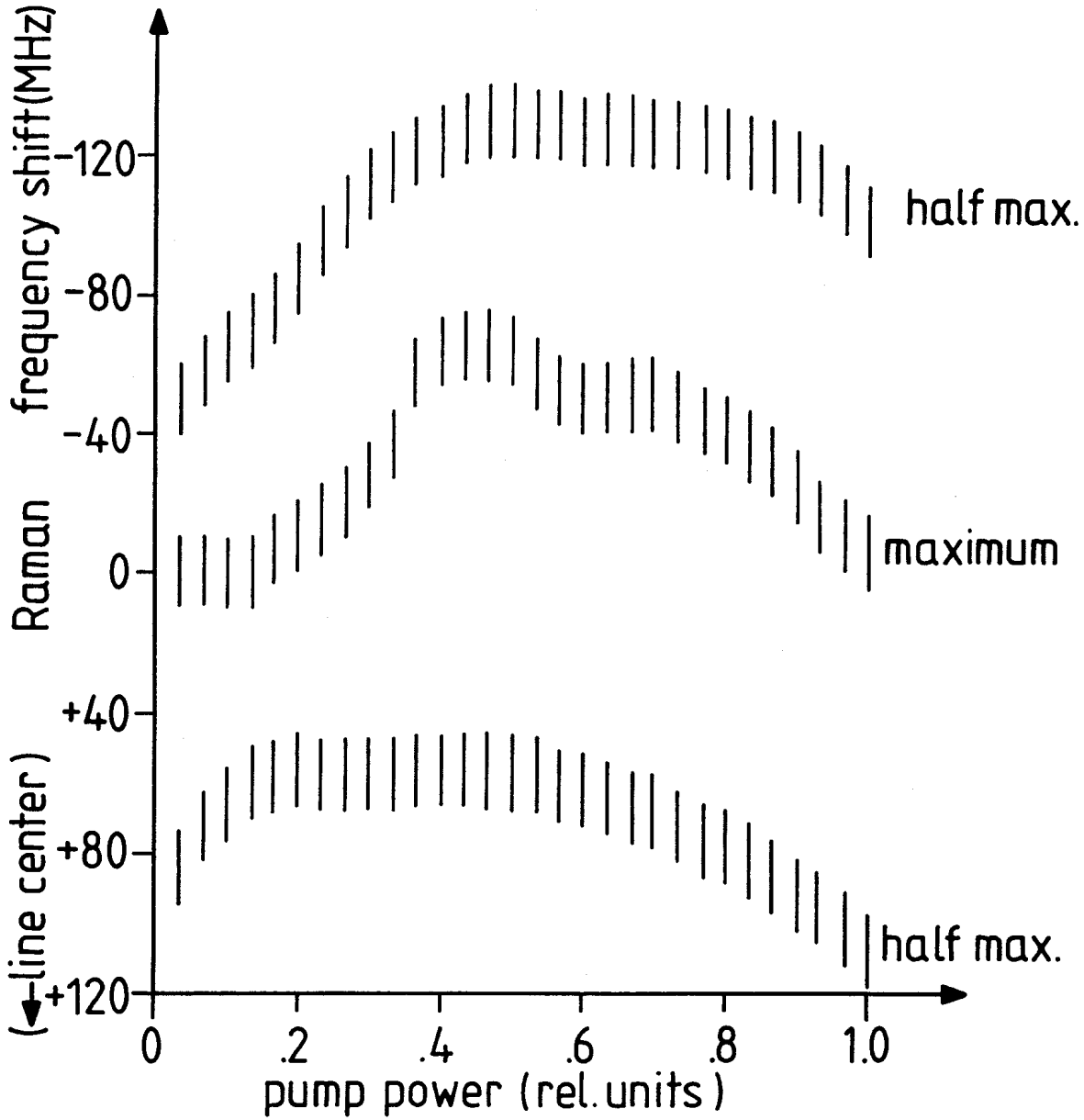
Raman frequency shift(MHz)
(-line center)
-120
-80
-40
0
+40
+80
+120
half max.
maximum
half max.
0
.2
.4
.6
.8
1.0
pump power (rel. units)

Fig. 8

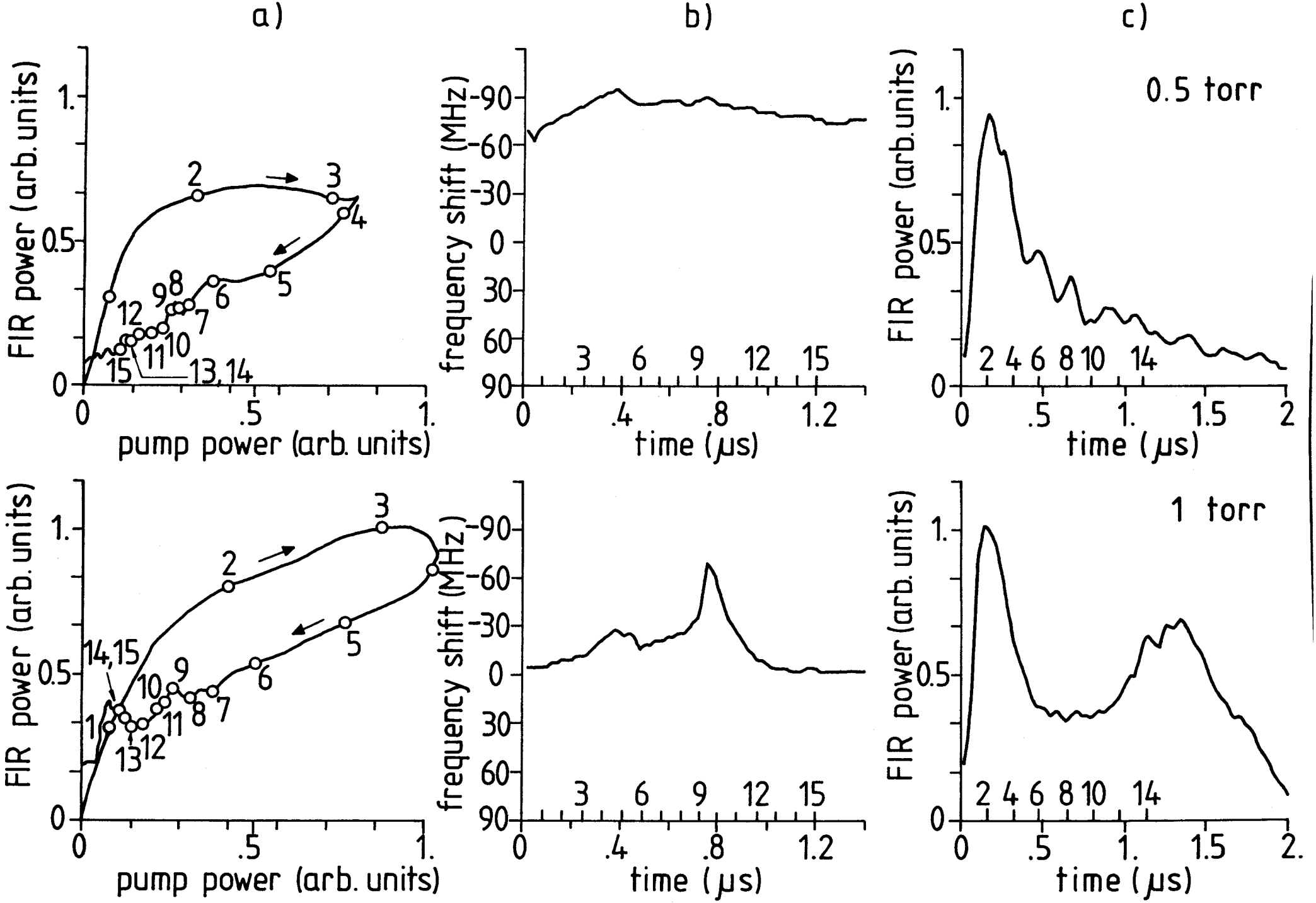
a)
b)
c)
FIR power (arb.units)
pump power (arb. units)
frequency shift (MHz)
time (μs)
0.5 torr
1 torr
1.
0.5
0
.5
1.
-90
-60
-30
0
30
60
90
.4
.8
1.2
1.5
2
2.
3
6
9
12
15
2 4 6 8 10 14
1
2
3
4
5
6
7
8
9
10
11
12
13
14,15

Fig. 9a

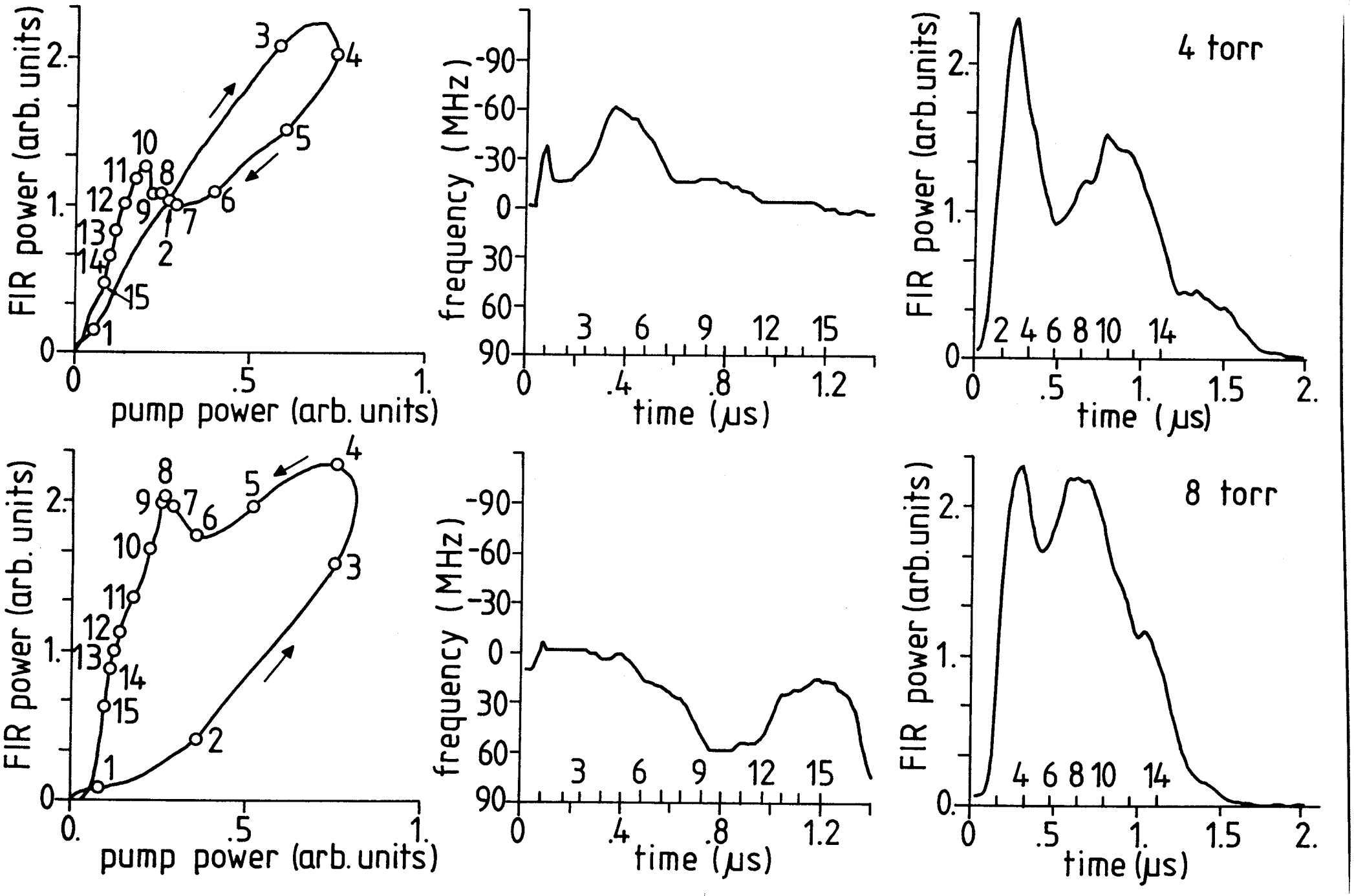
FIR power (arb. units)
pump power (arb. units)
frequency (MHz)
time (μs)
4 torr
8 torr

Fig. 9 b

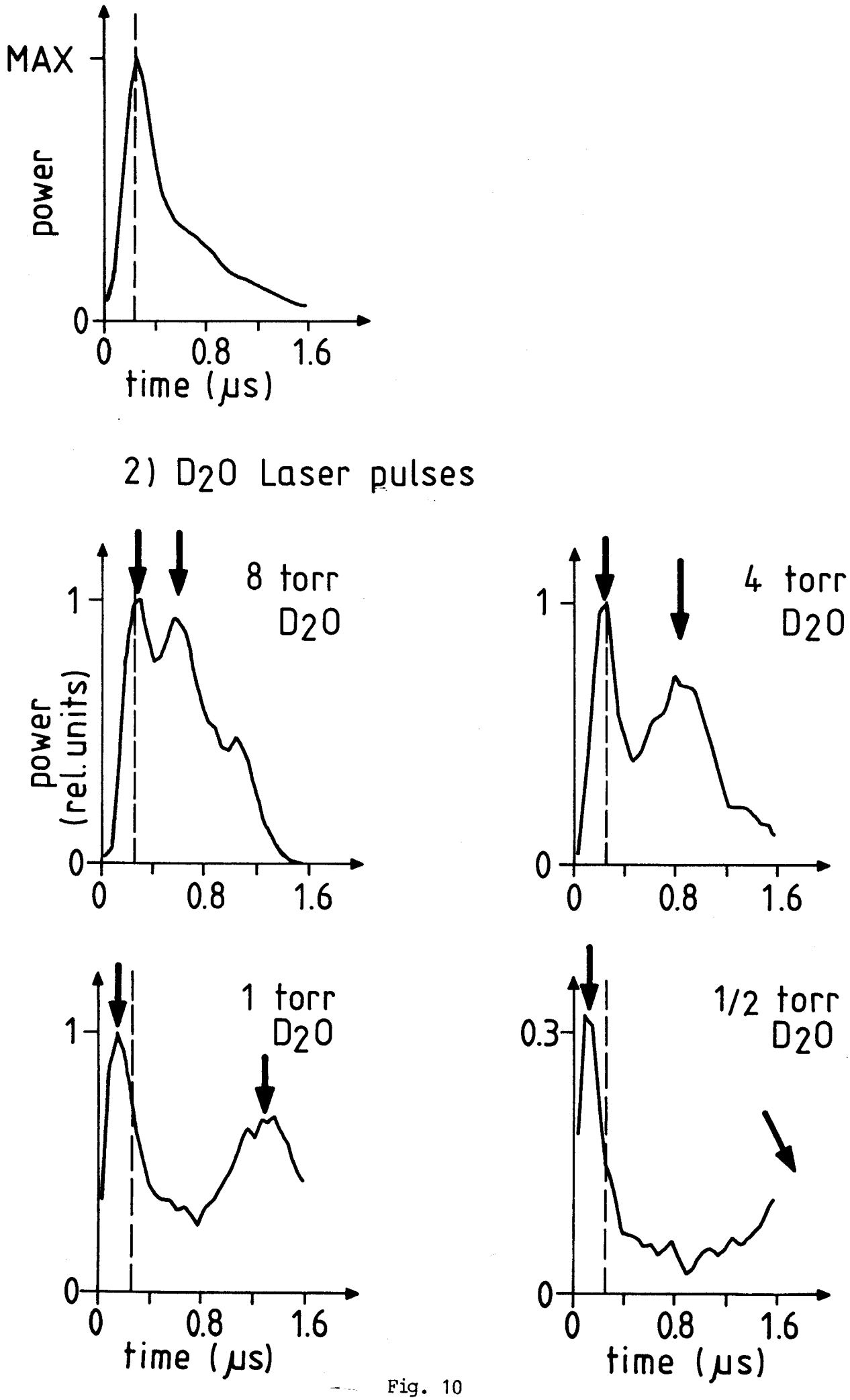
1) CO_2 Laser pulse
MAX
power
0
0
0.8
1.6
time (μs)
2) D_2O Laser pulses
8 torr
D_2O
power
(rel. units)
1
0
0
0.8
1.6
4 torr
D_2O
1
0
0
0.8
1.6
1 torr
D_2O
1
0
0
0.8
1.6
time (μs)
1/2 torr
D_2O
0.3
0
0
0.8
1.6
time (μs)

Fig. 10

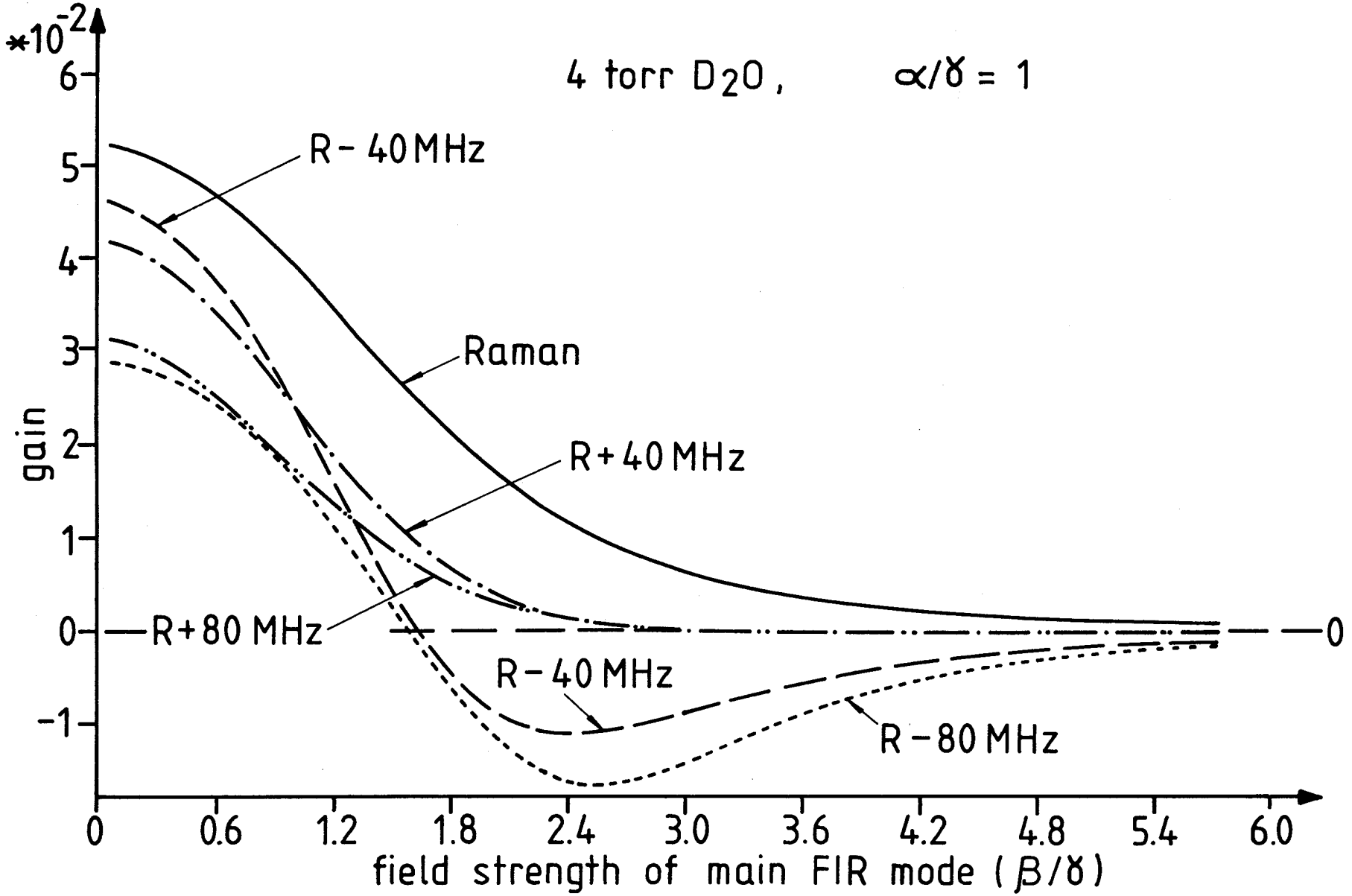
*10^-2
6
5
4
3
2
1
0
-1
gain
4 torr D2O, α/γ = 1
R - 40 MHz
Raman
R + 40 MHz
R + 80 MHz
R - 40 MHz
R - 80 MHz
0
0
0.6
1.2
1.8
2.4
3.0
3.6
4.2
4.8
5.4
6.0
field strength of main FIR mode (β/γ)

Fig. 11

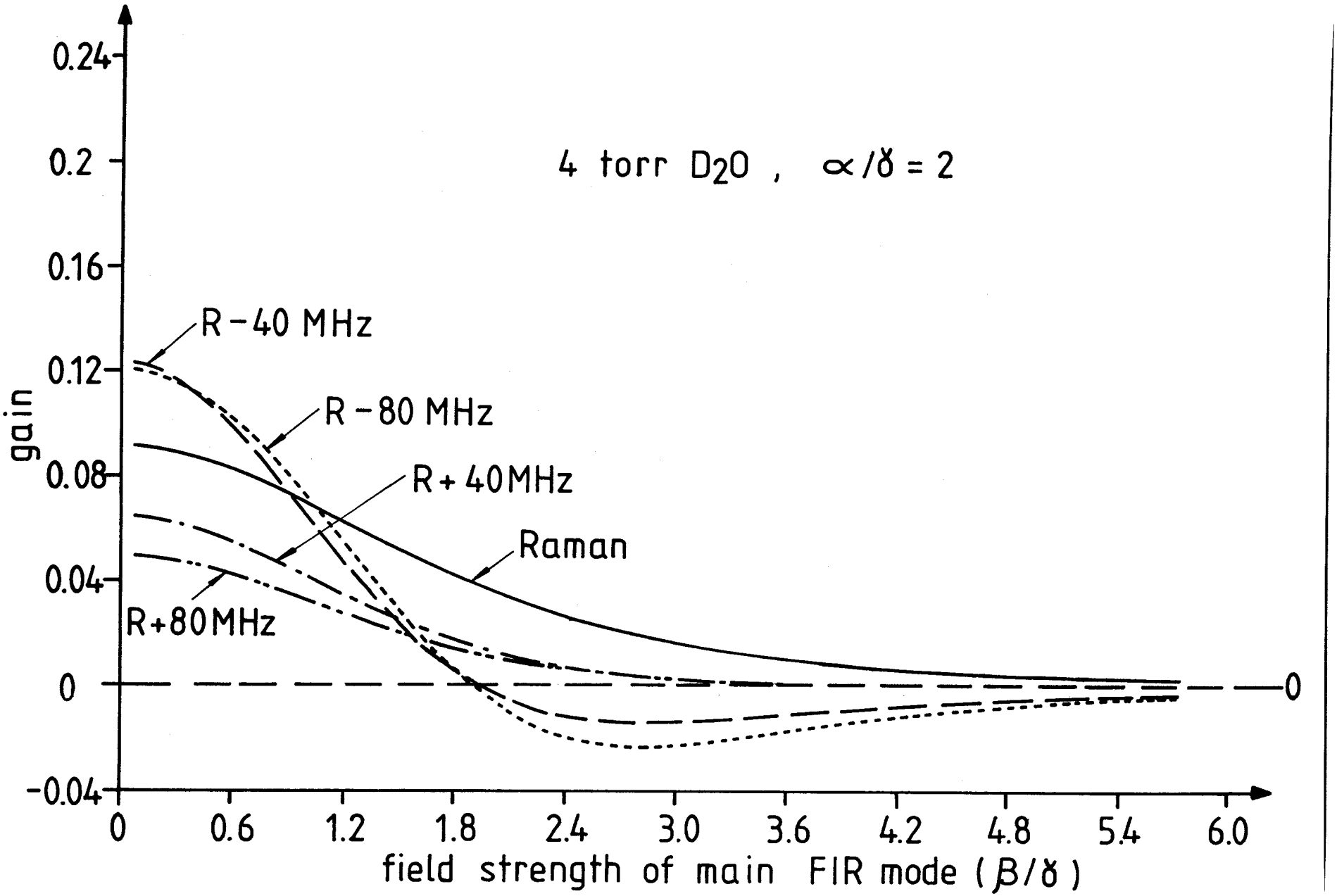
4 torr D_2O , $\alpha/\delta = 2$
0.24
0.2
0.16
0.12
0.08
0.04
0
-0.04
gain
R - 40 MHz
R - 80 MHz
R + 40 MHz
Raman
R + 80 MHz
0
0.6
1.2
1.8
2.4
3.0
3.6
4.2
4.8
5.4
6.0
field strength of main FIR mode (β/δ)

Fig. 12

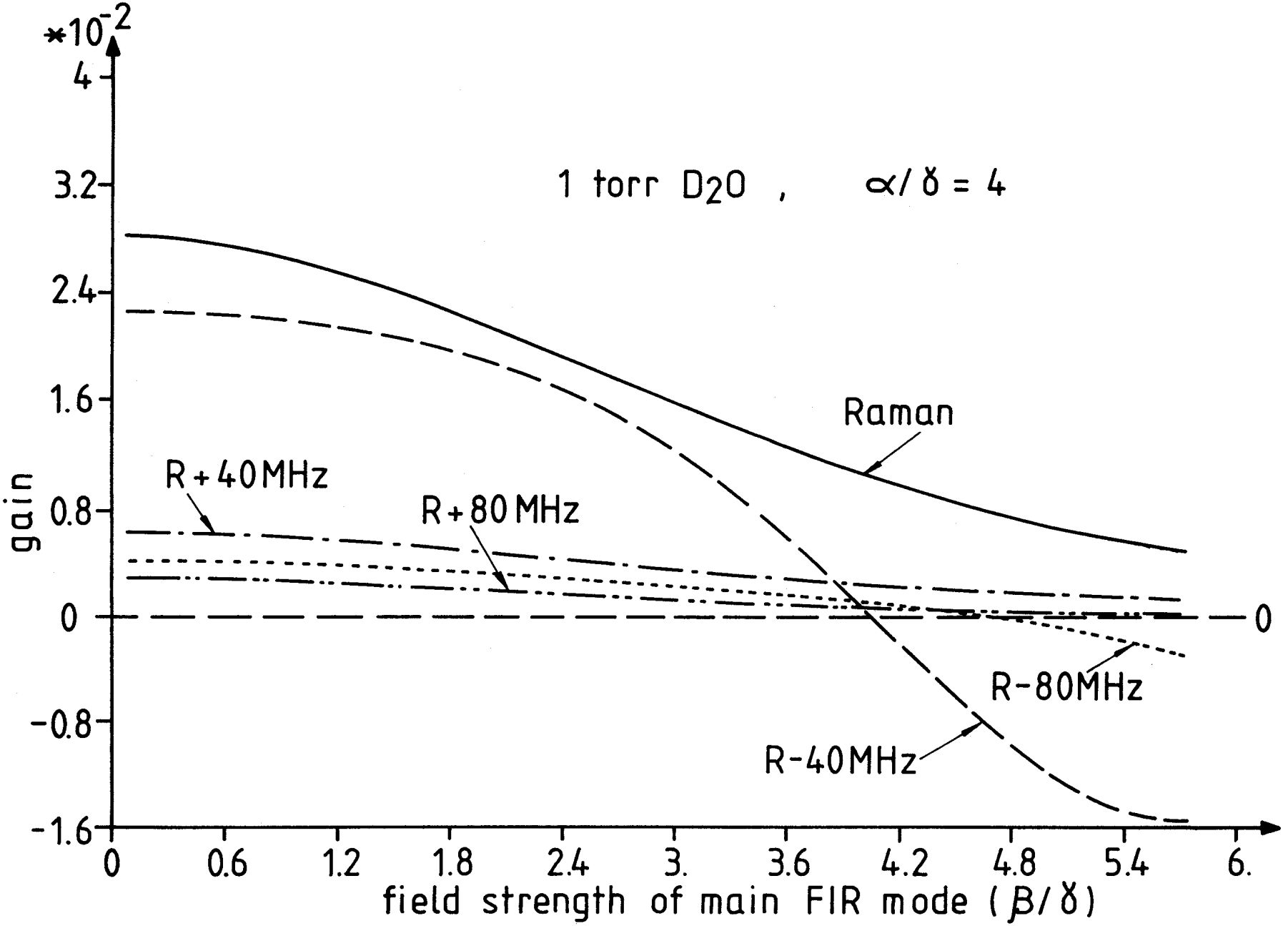
*10^-2
4
3.2
2.4
1.6
0.8
0
-0.8
-1.6
gain
1 torr D2O , α/δ = 4
Raman
R+40MHz
R+80MHz
R-80MHz
R-40MHz
0
0
0.6
1.2
1.8
2.4
3.
3.6
4.2
4.8
5.4
6.
field strength of main FIR mode (β/δ)

Fig. 13

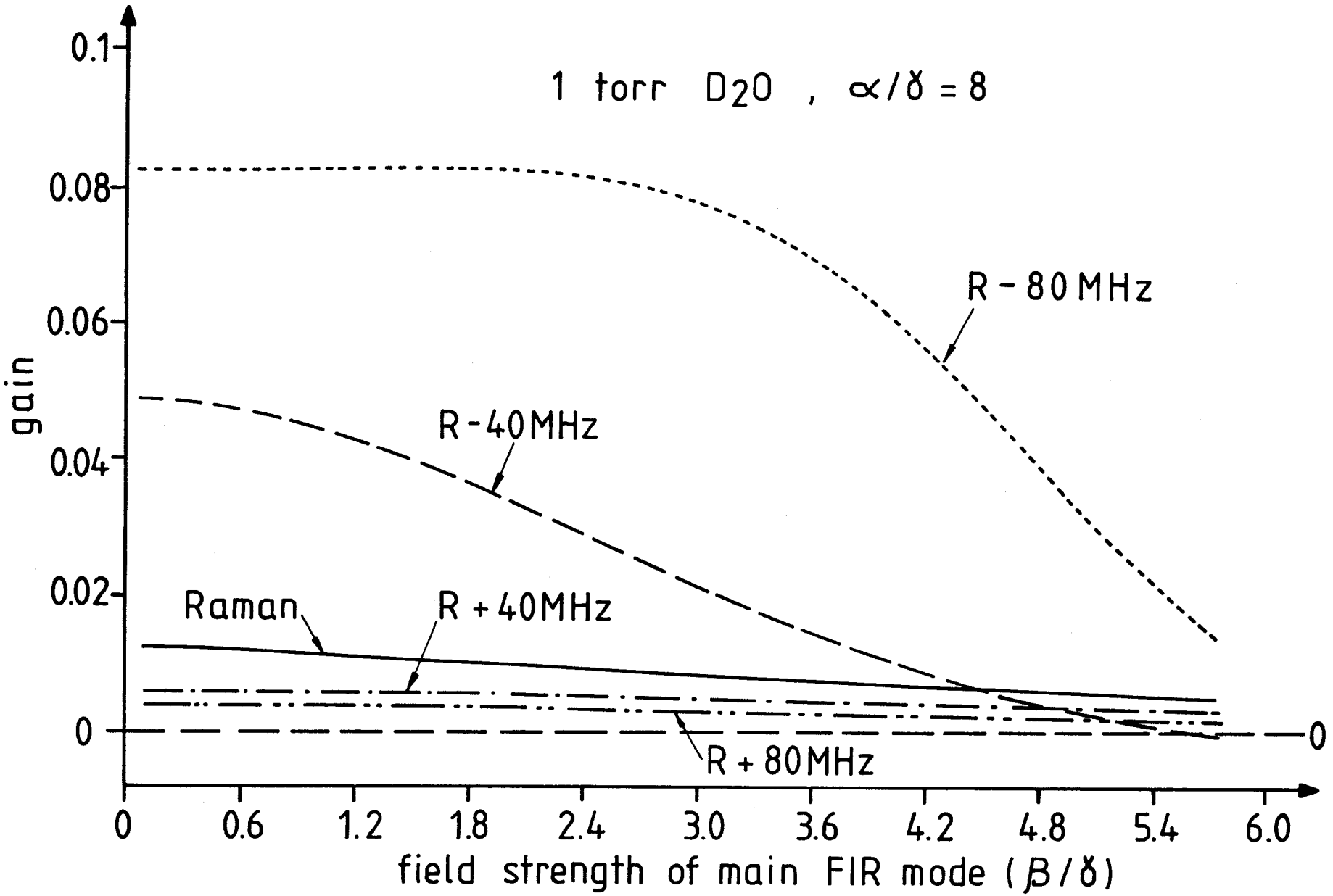
1 torr D_2O , $\alpha/\delta = 8$
0.1
0.08
0.06
0.04
0.02
0
gain
R - 80 MHz
R - 40 MHz
Raman
R + 40 MHz
R + 80 MHz
0
0
0.6
1.2
1.8
2.4
3.0
3.6
4.2
4.8
5.4
6.0
field strength of main FIR mode (β/δ)

Fig. 14